





CASE REPORT

Three-dimensional and catheter-based intracardiac echocardiographic characterization of the interatrial septum in 2 horses with suspicion of a patent foramen ovale

Ingrid Vernemmen¹  | Ellen Paulussen¹  | Julie Dauvillier² |
Annelies Declodt¹  | Gunther van Loon¹ 

¹Equine Cardioteam Ghent University, Department of Large Animal Internal Medicine, Faculty of Veterinary Medicine, Ghent University, Ghent, Belgium

²Vet Inside, Equine Internal and Sports Medicine Referral Practice, Sainte-Terre, France

Correspondence

Ingrid Vernemmen, Equine Cardioteam, Department of Large Animal Internal Medicine, Faculty of Veterinary Medicine, Ghent University, Salisburylaan 133, 9820 Merelbeke, Belgium.
Email: ingrid.vernemmen@ugent.be

Funding information

Fonds Wetenschappelijk Onderzoek, Grant/Award Number: 1556217N

Abstract

This case report describes the 2-dimensional transthoracic (2D-TTE), 3-dimensional transthoracic (3D-TTE) and intracardiac echocardiographic (ICE) characterization of the *fossa ovalis* region in 2 horses. The first case was presented for poor performance and showed an anechoic zone in the interatrial septum on 2D-TTE. Based on 3D-TTE a deepened *fossa ovalis* could be identified and using ICE the presence of an interatrial shunt could be excluded. The second case was referred for a cardiac murmur and the presence of turbulent flow in and around the interatrial septum on 2D-TTE color flow Doppler. The complementary use of 2D-TTE, 3D-TTE, and ICE allowed detailed characterization of a patent *foramen ovale*, with evidence of a left-to-right shunt in a dorsocranial to ventrocaudal direction with limited hemodynamic implications. These 2 cases underline the feasibility of 3D-TTE and ICE in horses and especially show the added value of ICE in a clinical setting.

KEYWORDS

cardiology, equine, fossa ovalis, left-to-right shunt, ultrasound

1 | CASE DESCRIPTION

1.1 | Case 1

A 9-year-old, 670 kg Friesian gelding used for dressage was admitted at the Equine Cardioteam, Ghent University for evaluation of chronic exercise intolerance. As a foal, the horse had been hospitalized for dyspnea. At admission, no abnormalities were identified on physical examination. Based on the history of exercise-induced tachypnea,

thoracic radiographs, airway endoscopy, a lunging exercise test¹ and bronchoalveolar lavage were performed and inflammatory airway disease was diagnosed. However, to exclude cardiac pathology, echocardiography and electrocardiography were performed. On 2-dimensional transthoracic echocardiography (2D-TTE) (Vivid E95, 4VC probe, GE Healthcare, Diegem, Belgium) cardiac dimensions were within reference ranges² and no valvular regurgitations were detected. A round anechoic area representing the part of the *fossa ovalis* underneath the limbus was identified, but the *fossa ovalis* seemed to be open towards the left atrium (LA) (Figure 1). Some turbulent flow was present in the *fossa ovalis*, associated with a vibrating hyperechoic line at the right atrial (RA) side of the septum. However, color flow Doppler was not conclusive in diagnosing an interatrial

Abbreviations: 2D-TTE, 2-dimensional transthoracic echocardiography; 3D-TTE, 3-dimensional transthoracic echocardiography; APD, atrial premature depolarization; ECG, electrocardiogram; ICE, intracardiac echocardiography; LA, left atrium; PFO, patent foramen ovale; RA, right atrium.

This is an open access article under the terms of the [Creative Commons Attribution-NonCommercial-NoDerivs](https://creativecommons.org/licenses/by-nc-nd/4.0/) License, which permits use and distribution in any medium, provided the original work is properly cited, the use is non-commercial and no modifications or adaptations are made.

© 2022 The Authors. *Journal of Veterinary Internal Medicine* published by Wiley Periodicals LLC on behalf of American College of Veterinary Internal Medicine.

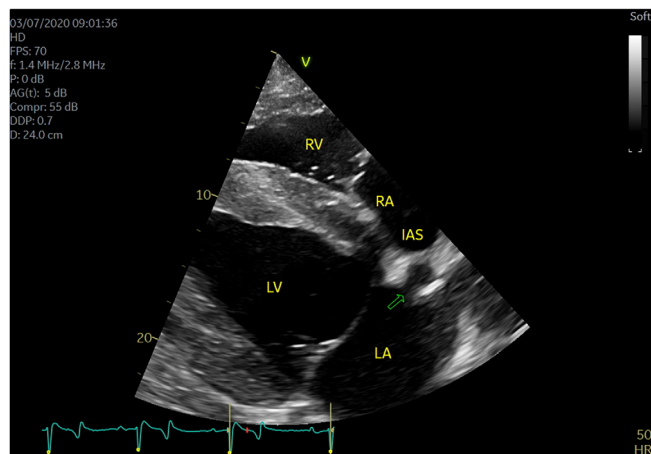


FIGURE 1 Case 1: Right parasternal long-axis (4-chamber) view focused on the left atrium showing an anechoic area in the interatrial septum that appears to connect to the left atrium (green arrow). IAS, interatrial septum; LA, left atrium; LV, left ventricle; RA, right atrium; RV, right ventricle

communication, as the turbulent flow could also have been caused by flow entering from the caudal *vena cava* (Figure 2). Three-dimensional transthoracic echocardiography (3D-TTE) (Vivid E95, 4VC probe, GE Healthcare, Diegem, Belgium; settings: 1.7 MHz/3.3 MHz, 34 frames per second [FPS], 21.8 cm imaging depth, single-beat acquisition) of the region of the *fossa ovalis* was acquired as follows: starting from the 4-chamber view on 2D-TTE, the probe was angled slightly more caudally to visualize the *fossa ovalis*, after which the region of the *fossa ovalis* was selected to create a focused 3D volume. During post-processing, the 3D volume was rotated so that the top on screen was dorsal and left on screen was caudal, thus creating an en-face view of the *fossa ovalis* when looking from within the right atrium. This showed a deepened *fossa ovalis* (Figure 3A and Video S1, Supporting Information). Because of the limited spatial resolution of the image, and considering that voxel drop-out on 3D-TTE is also commonly found in normal horses (Figure 3B,C), it remained unclear if there was a communication between the atria. Intracardiac echocardiography (ICE) was performed to exclude an interatrial communication with increased certainty. After sedation, the caudal part of the right jugular vein region was clipped and surgically prepared. A 9 French introducer sheath (Intro-Flex, Edward Lifesciences, Irvine, California) was placed, allowing the introduction of the 8 French steerable ICE catheter (phased-array, 5.0-10.0 MHz, ACUSON AcuNav ultrasound catheter, Biosense Webster, Johnson and Johnson, Diegem, Belgium). After connection with the ultrasound device (Vivid IQ, GE Healthcare, Diegem, Belgium), the ICE catheter was advanced with the probe facing ventrally until the RA, tricuspid valve and RA appendage came into view (settings: 8.0 MHz, 32 FPS, 12 cm imaging depth). In order to advance the ICE probe to the *fossa ovalis* region, the prominent intervenous tubercle was passed by following the curvature of the tubercle, with subsequent gentle retroflexion of the catheter around the tubercle. Caudal to the intervenous tubercle, the catheter was straightened and the *fossa ovalis* was brought into view through

90° counterclockwise rotation of the ICE catheter (Figure 4). Gentle clockwise and counterclockwise rotation (total range of 120°) allowed detailed inspection from the most ventral to the most dorsal part of the *fossa ovalis*, respectively. The examination showed that the *fossa ovalis* was closed. Using intracardiac color flow Doppler, a communication could be excluded with increased certainty (Video S2). The electrocardiogram (ECG), with modified base-apex electrode-positioning (Televet 100, Engel Engineering Services GmbH, Offenbach an Main, Germany), revealed 269 atrial premature depolarizations (APD) during 2D-TTE and 3D-TTE, and 273 APDs during ICE. Cardiac troponin I concentrations were normal (ref. <0.06 ng/mL).

A cardiac origin was excluded as the cause of the clinical signs, and treatment for inflammatory airway disease was instigated, and included corticosteroid treatment (0.03 mg/kg BW dexamethasone IV for 2 days, followed by 1 mg/kg BW prednisolone PO for 21 days, followed by 1 mg/kg BW prednisolone every other day for 10 days), oral clenbuterol (0.8 µg/kg BW BID for 4 weeks), inhaled salbutamol (1 µg/kg BW every 4 hours for 10 days) and measures to reduce environmental dust. One year later, the management of the exercise intolerance remained challenging. The horse was retired and no further examinations concerning the exercise intolerance were performed.

1.2 | Case 2

A 4-year-old 567 kg French Warmblood gelding in training for show jumping was referred for evaluation of a suspected interatrial communication. A holosystolic murmur had been detected during a period of colic a year before, and confirmed upon 2 successive cardiac auscultations. There was no available information about cardiac auscultation beforehand. Echocardiography by the referring veterinarian revealed moderate mitral regurgitation, mild aortic regurgitation and turbulent flow in and around the interatrial septum. In addition, right ventricular dilation and decreased left ventricular systolic function were detected. The horse was referred for further evaluation.

Physical examination at admission revealed no abnormalities, except for a grade 4/6 holosystolic plateau-type murmur and a grade 2/6 holodiastolic decrescendo murmur on the left side, and a grade 2/6 holosystolic plateau-type murmur on the right side. At rest (ECG duration of 1 hour during 2D- and 3D-TTE), only 1 APD was present and no ECG abnormalities were seen during a lunging exercise test. On 2D-TTE,² slight dilation of the left and right ventricle were seen, as well as a slightly decreased left ventricular ejection fraction (64%), moderate mitral regurgitation and mild aortic regurgitation. An anechoic zone of 1.5 cm diameter was present in the interatrial septum (Figure 5A) with abnormal turbulent flow on color flow Doppler. The anechoic zone revealed to be in the region of the *fossa ovalis* on simultaneous multiplane imaging (Figure 5B). Continuous wave Doppler revealed a systolic left-to-right flow with a maximum velocity of 2.03 m/s (pressure gradient of 16 mmHg). Pulmonary-to-systemic flow ratio ($Q_p : Q_s$), based on pulsed-wave Doppler of the pulmonary³ and aortic flow,⁴ was 1.8:1. Agitated saline administration did not show right-to-left shunting and negative contrast, which can often be

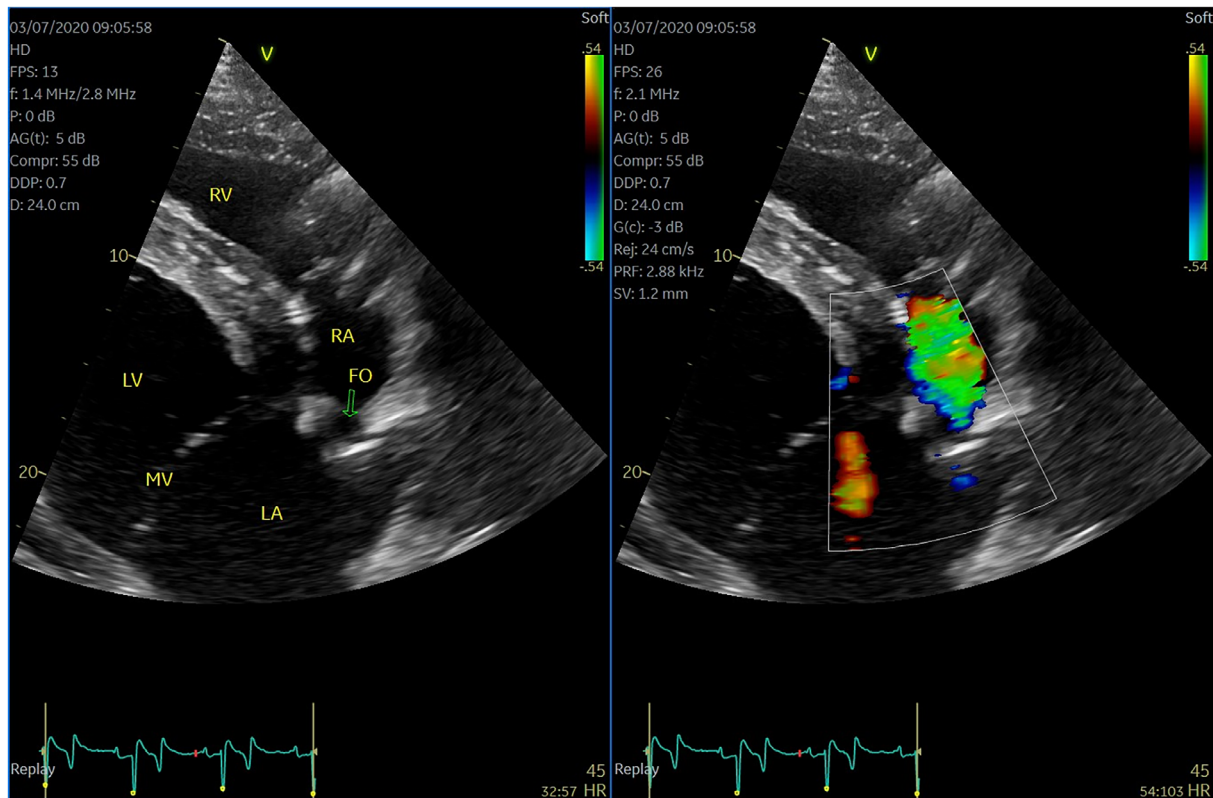


FIGURE 2 Case 1: Two-dimensional transthoracic echocardiography: Right parasternal long-axis (4-chamber) view in diastole focused on the fossa ovalis (green arrow). Color flow Doppler of the region showed turbulent flow from the caudal vena cava, which made it challenging to determine the presence of a shunt. FO, fossa ovalis; LA, left atrium; LV, left ventricle; MV, mitral valve; RA, right atrium; RV, right ventricle

detected with a left-to-right shunt, could not be identified. Using 3D-TTE (Vivid E95, 4VC probe; settings: 1.7 MHz/3.3 MHz, 22 FPS, 23 cm imaging depth, single-beat acquisition; image acquisition and postprocessing similar to Case 1), the interatrial communication could be identified as a patent foramen ovale (PFO), characterized by the presence of an intact *septum primum* and *secundum* but lack of functional closure of the *ostium secundum* (Figure 6). The PFO had a diameter of 1.5 cm at the LA side and of 2.2 cm at the RA side, measured on 2D tomographic orthogonal slices of the 3D volume. Using 3D color flow Doppler, the left-to-right flow trajectory, starting dorsocranially at the left side of the PFO and running in a ventrocaudal direction to the right side of the PFO, could be visualized (Video S3), despite the fact that the final image resolution was lower compared to the 2D-TTE image. In the sedated horse, ICE examination was performed to acquire more detail of the interatrial septum (settings: 6.0 MHz, 57 FPS, 16.0 cm imaging depth). Preparation was performed as described in the previous case. First, the most dorsal part of the PFO region was visualized through $\pm 150^\circ$ counterclockwise rotation, recognized by the bifurcation of ostium III of the pulmonary veins which is located dorsal to the interatrial septum.⁵ By slow clockwise rotation over 120° , thus scanning the PFO from dorsocranial to ventrocaudal, it could be clarified that the PFO opening was situated dorsocranially, deep underneath the limbus, and resulted in a continuous (systolic and diastolic) flow running in ventrocaudal direction

entering the RA. The presence of an intact *septum primum* and *secundum* could be visualized in detail, thus differentiating from an atrial septal defect (Figure 7 and Videos S4 and S5). One-dimensional measurement of the defect based on ICE yielded similar results as the multidimensional 3D-TTE measurement. During ICE examination, 29 APDs were present.

It was concluded that the left-sided systolic murmur was caused by the mitral regurgitation and the diastolic murmur by the aortic regurgitation. The right-sided systolic murmur was probably caused by the interatrial left-to-right shunt. Theoretically, moderate mitral regurgitation might have resulted in increased LA systolic pressure⁶ and shunt volume, which could have contributed to right ventricular dilation, but invasive pressure measurements were not performed. Occluder implantation was considered but not performed: as the PFO opening was located deep underneath the limbus full deployment of the occluder could be hampered and the risk for device dislodgement would be increased. Furthermore, flow through the PFO was limited and only left-to-right. No explanation was found for the mildly decreased left ventricular ejection fraction, however this value was borderline and therefore presumably clinically irrelevant. The horse was allowed to continue competition and a follow-up examination within 1 year showed no increase in PFO size, stable valvular regurgitations and similar ventricular size and function. The horse was allowed to continue training and competition, with yearly follow-up.

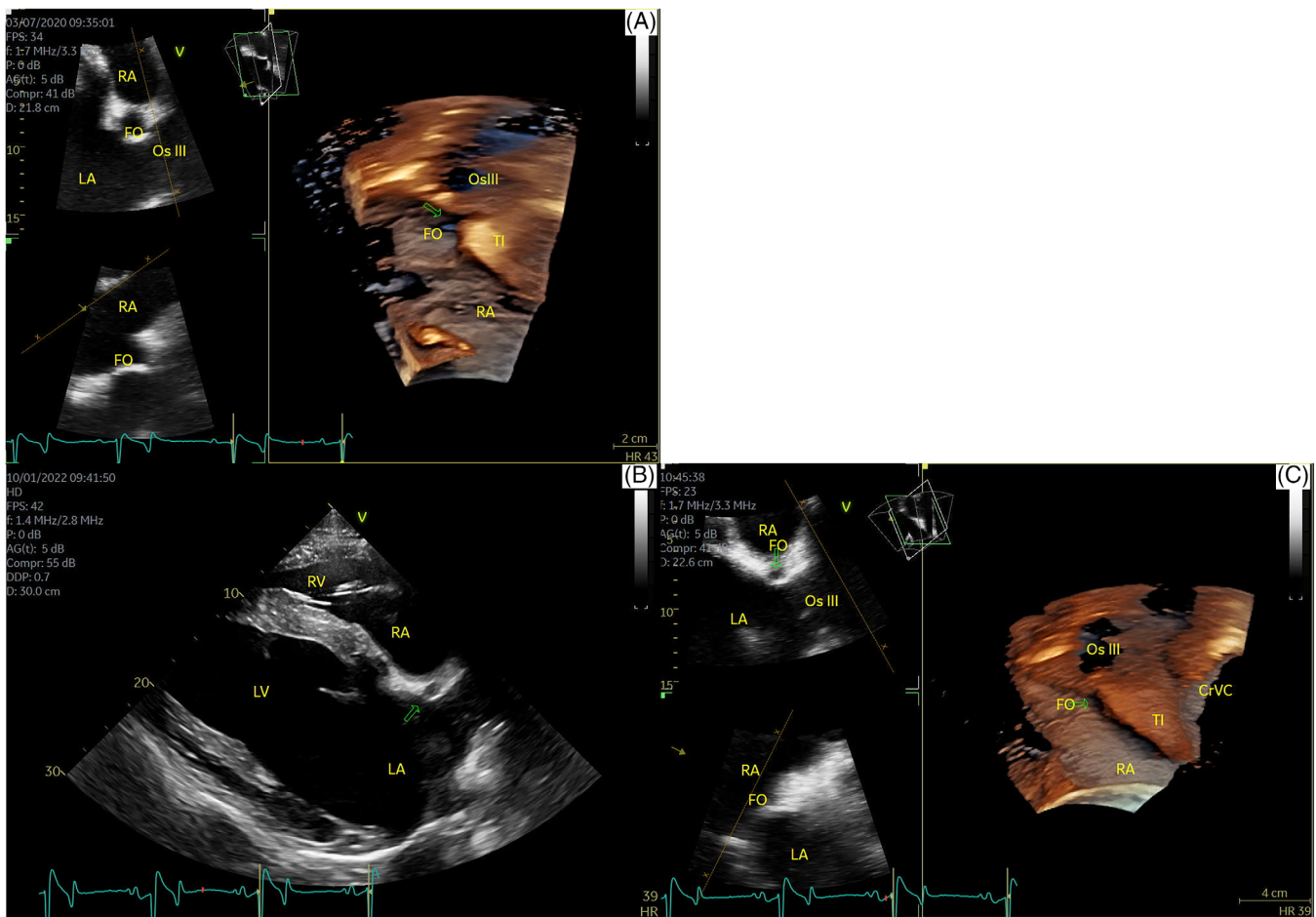


FIGURE 3 Case 1: (A) Right parasternal long-axis view acquired with 3-dimensional echocardiography optimized for the region of the *fossa ovalis* (right) with corresponding orthogonal 2-dimensional sections (left), and the orientation of the 2D images in relation to the 3D volume (center top figure). View from within the right atrium looking at the interatrial septum; left is caudal, top is dorsal. A deep *fossa ovalis* can be seen, with drop-out of voxels in the deepest part of the fossa (green arrow). Images taken in a horse with a normal interatrial septum: (B) Two-dimensional transthoracic echocardiographic right parasternal long-axis (4-chamber) view and (C) right parasternal short-axis view acquired with 3-dimensional echocardiography optimized for the region of the *fossa ovalis* (right) with corresponding orthogonal 2D sections (left), and the orientation of the 2D images in relation to the 3D volume (center top figure). View from within the right atrium looking at the interatrial septum; left is caudal, top is dorsal. Also in this horse, an anechoic zone, but without apparent connection to the left atrium, is visible on the 4-chamber view (green arrow) and drop-out of voxels in the region of the *fossa ovalis* can be seen on 3D echocardiography (green arrow). AO, aorta; CaVC, caudal vena cava; CrVC, cranial vena cava; FO, *fossa ovalis*; LA, left atrium; LV, left ventricle; Os III, ostium III of the pulmonary veins; RA, right atrium; RV, right ventricle; TI, *tuberculum intervenosum*

2 | DISCUSSION

This case report describes the use of a combination of echocardiographic modalities to characterize morphological variations of the interatrial septum and estimate their clinical relevance. Two-dimensional TTE has the advantage of providing a comprehensive qualitative and quantitative assessment of cardiac dimensions, structure and function. However, correlating the 2D image with the cardiac anatomy remains challenging, especially when examining morphological abnormalities. The recent advent of real-time 3D-TTE in equine cardiology solves this issue, as instead of a 2D slice, a 3D volume is acquired using a matrix-array transducer, thus gaining insight into the 3D conformation of cardiac structures. Clinical use of 3D-TTE has been reported for the evaluation of the aortic valve and an atrial

septal defect.^{7,8} Left atrial volumetric assessment by 3D-TTE is also gaining attention for use in horses.⁹ A disadvantage is that 3D-TTE suffers from the trade-off of spatial and temporal resolution. Temporal resolution can be increased by acquisition over multiple beats but this might result in stitching artifacts because of horse, breathing and probe movement. Multibeat acquisition cannot be used in case of arrhythmias, such as atrial fibrillation or second degree atrioventricular block.^{9,10} Depending on the resulting 3D image quality, post-processing might be needed for image optimization and is software-dependent. In our cases, this was limited to changing gain-settings, viewing angle and increasing brightness and contrast. A prerequisite for qualitative 3D imaging is sufficient 2D image quality, which can be challenging to obtain in broad-chested or overweight horses.¹¹ Transthoracic echocardiography also has the disadvantage of being limited

by the intercostal spaces and lung field and only low frequencies can be used for sufficient imaging depth, resulting in lower spatial resolution.^{11,12}

These restrictions are overcome by ICE. This minimally invasive imaging technique is performed using a phased-array ultrasound probe mounted on the tip of a 8-12.5 French steerable catheter providing a 2D or 3D image with up to 16 cm imaging depth (depending on the manufacturer). Functionalities such as color Doppler, tissue Doppler, 2D speckle tracking and integration with a 3D mapping system are increasingly available. Via a venous introducer, the ICE probe can be navigated towards the heart using mechanical steering and

rotation.^{13,14} Hence, the technique does not suffer from body conformation and provides detailed imaging with high resolution.¹⁵ However, this can make interpretation challenging and contributes to the steep learning curve. Additional disadvantages include movement of the catheter during image acquisition, induction of transient arrhythmias, cost of the catheter and need for a minimally invasive venous entry.¹⁵ In human medicine, ICE is commonly used in interventional cardiology for adequate guidance of, for example, endocardial ablation, transseptal puncture for LA access, or percutaneous intracardiac defect closure.^{15,16} In dogs, ICE is mainly applied in experimental settings,¹⁷⁻¹⁹ with only a few clinical reports.^{20,21} The use of ICE in horses remains anecdotal.²²⁻²⁴

In our 2 cases, the complementary use of 3D-TTE and ICE, in addition to the standard 2D-TTE, provided deeper insight into the interatrial septal morphology. In Case 1, 3D-TTE allowed for better understanding of the conformation of the *fossa ovalis*, but an atrial communication could not be excluded because of voxel dropout which is a common issue in 3D-TTE.¹⁰ Because of incoming turbulent blood flow from the caudal *vena cava*, which is commonly found in the normal horse,²⁵ color flow Doppler was not conclusive. Using ICE, the anomalous morphology of the region of the *fossa ovalis* could be imaged in detail without interference of body conformation, and a communication could be excluded. In Case 2, 3D-TTE was additionally useful to better assess defect size, as the measurements can be performed independently of probe alignment in relation to the lesion.²⁶ Using ICE, the transthoracic findings could be confirmed with increased detail and device closure possibilities could be assessed. In both cases, except for transient APDs, ICE could be performed without any complications.

A PFO results from incomplete closure of the *foramen ovale* after birth and should therefore not be regarded as a congenital defect and

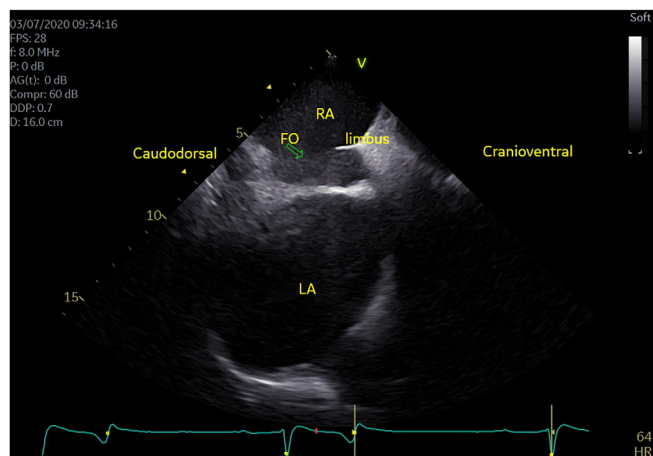


FIGURE 4 Case 1: Intracardiac echocardiography of the region of the *fossa ovalis*; left is caudodorsal, top is right lateral. A deep *fossa ovalis* (green arrow) can be seen, with no visible connection to the left atrium. FO, *fossa ovalis*; LA, left atrium; RA, right atrium

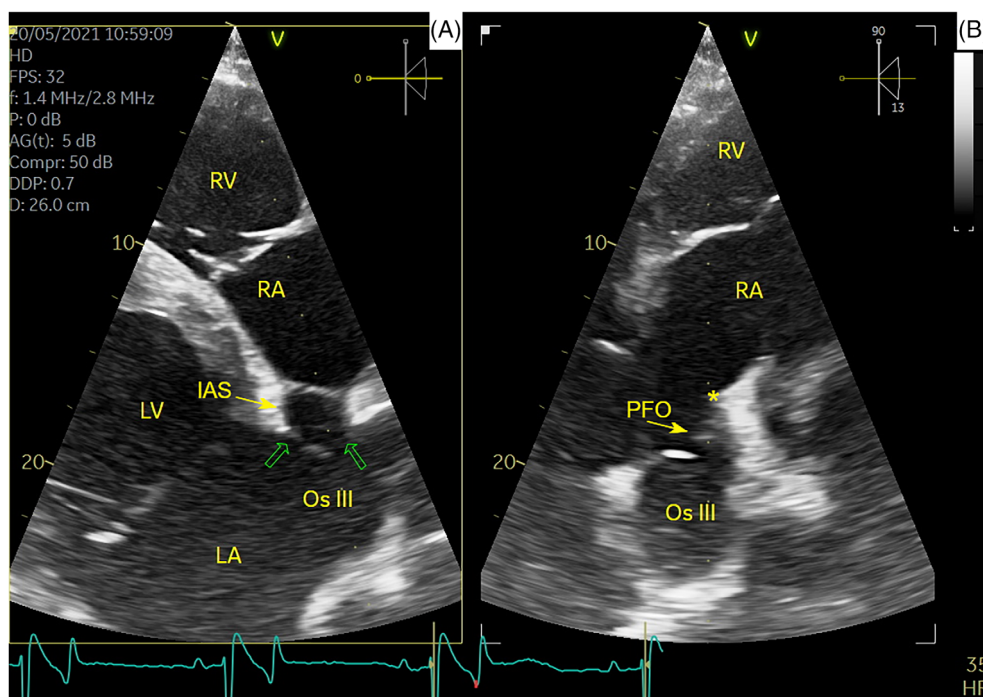


FIGURE 5 Case 2: (A) Right parasternal long-axis (4-chamber) view focused on the left atrium showing an anechoic area in the interatrial septum (green arrows) with (B) orthogonal cross-section of the 4-chamber view at the level of the yellow dotted line, indicating that the location of the anechoic area is situated in the region of the *fossa ovalis* revealing a patent *foramen ovale*. *, limbus; IAS, interatrial septum; LA, left atrium; LV, left ventricle; Os III, ostium III of the pulmonary veins; PFO, patent *foramen ovale*; RA, right atrium; RV, right ventricle

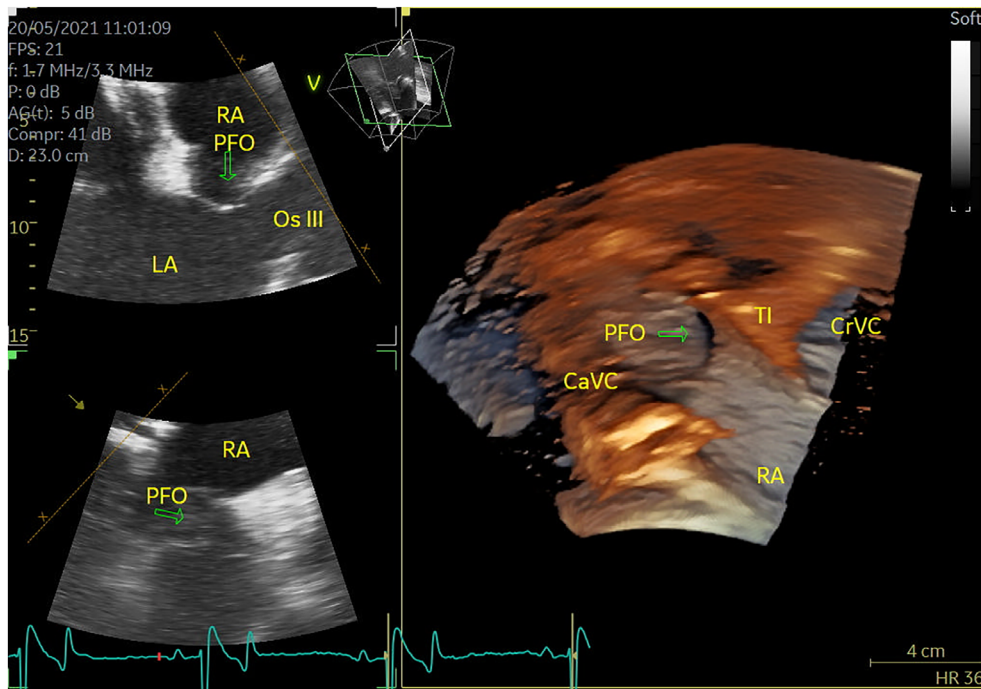


FIGURE 6 Case 2: Right parasternal long-axis view with 3-dimensional echocardiography optimized for the region of the fossa ovalis (right) with corresponding orthogonal 2-dimensional sections (left), and the orientation of the 2D images in relation to the 3D volume (center top figure). View from within the right atrium looking at the interatrial septum; left is caudal, top is dorsal. A patent foramen ovale (green arrow) with connection to the left atrium could be suspected. CaVC, caudal vena cava; CrVC, cranial vena cava; Os III, ostium III of the pulmonary veins; PFO, patent foramen ovale; RA, right atrium; TI, tuberculum intervenosum

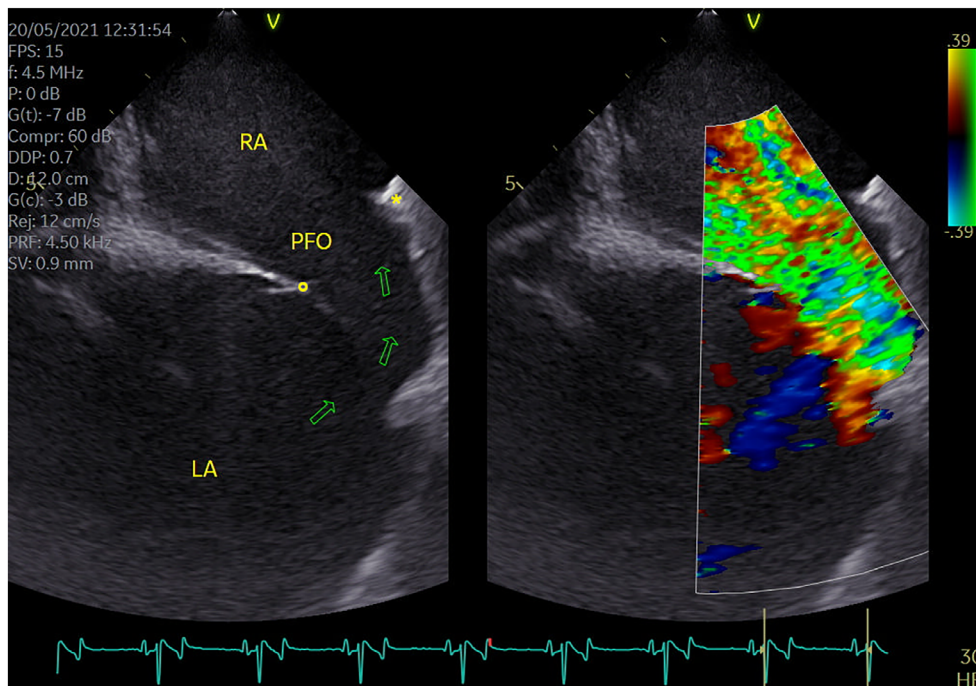


FIGURE 7 Case 2: Intracardiac echocardiography of the region of the fossa ovalis without (left panel) and with color flow Doppler (right panel); left is caudal, top is right lateral. The thinnest part of the fossa ovalis, the septum primum (°), and the muscular ridge of the septum secundum, the limbus (*), could be visualized in detail. Patency of the fossa ovalis could be identified (green arrows) and a shunt was confirmed by color flow Doppler. *, limbus; °, septum primum; LA, left atrium; PFO, patent foramen ovale; RA, right atrium

be distinguished from an atrial septal defect, which arises from a malformation of the interatrial septum during fetal development.²⁷⁻³⁰ In order to be able to differentiate both interatrial communications in the context of potential genetic predisposition, thorough understanding of the atrial septation process is necessary. The first component of the interatrial septum, the septum primum, grows from the atrial roof towards the endocardial cushions, leaving an interatrial communication between the septum primum and the endocardial cushions known as the ostium primum. Fenestrations arise in the caudal part of the septum primum in order to create the ostium secundum, while the septum

primum and endocardial cushions fuse, thus closing the ostium primum. Ingrowth of the atrial tissue on the RA side of the septum primum, that is, the septum secundum, allows right-to-left interatrial communication through the ostium secundum, while the septum primum acts as a 1-way valve of the ostium secundum to inhibit left-to-right shunting. This way, fetal oxygenated blood is led directly to the fetal tissues, instead of detouring past the nonfunctional lungs.^{8,28,29,31} In the different types of atrial septal defects, 1 or more septal components are absent or malformed, recognized by an abrupt interruption in the interatrial septum with evidence of interatrial communication on color

flow Doppler. In contrast, all septal components are present in a PFO but anatomical and functional closure does not take place. Echocardiographically this is recognized by the presence of both an intact *septum primum* (ie, the thinnest part of the *fossa ovalis*) and *secundum* (recognized by the muscular ridge that forms the limbus) and persistence of communication through the *ostium secundum*, as was seen on 3D-TTE and ICE in Case 2. Functional closure should happen in the first 48 hours because of increasing LA pressure, and anatomical closure should ensue in the following weeks.³² Elevated RA pressures and pulmonary hypertension, for example, caused by pulmonary disease, interfere with this physiological process and can eventually result in delayed closure or persistence of communication.²⁵ However, no data were available on the medical history of the horse as a foal in Case 2. Whether the neonatal dyspnea, which is known to cause elevation of RA pressures, might have influenced the *fossa ovalis* closure process in Case 1, remains unknown.

In the absence of cryptogenic stroke or other cardiac abnormalities, PFO is regarded as a normal anatomical variation in humans, with a prevalence of around 25%.²⁷ To the authors' knowledge, no reports exist describing the *ante mortem* diagnosis nor the clinical importance of a PFO in the adult horse. Atrial left-to-right shunts cause right-sided volume overload and lead to increased pulmonary artery flow and therefore increased pulmonary venous return, which can result in left-sided volume overload.^{8,25,33} Left-to-right shunts are regarded as important if the pulmonary-to-systemic flow ratio is higher than 1.8 : 1.²⁵ Therefore, the hemodynamic effect of the shunt was within functional limits in Case 2. However, reliability of transthoracic echocardiographic flow measurements is limited in horses because of the angle-dependency of the measurements and the inaccuracies in the determination of the vessel diameter and flow areas.^{25,34} Right-to-left shunts on the other hand cause arterial hypoxemia and general tissue hypoxia²⁵ and carry the risk of passage of undiluted intravenous medication or accidental intravenous air bubble injection into the arterial circulation.³⁵ In Case 2, a left-to-right shunt became evident on 2D-TTE, 3D-TTE, and ICE color flow Doppler and no right-to-left communication could be shown using agitated saline. In selected cases of cryptogenic stroke in human medicine, PFO closure is considered and mainly performed with percutaneous occluder devices.³⁶ In dogs, no reports of PFO closure exist to the authors' knowledge; however, transcatheter closure of atrial septal defects is performed occasionally.^{37,38} Percutaneous occluder implantation has been reported in horses for treatment of aorto-cardiac fistula,^{39,40} but indications, feasibility, and clinical outcome for closure of PFOs and atrial septal defects are still to be investigated.

In conclusion, these cases show the added value of 3D-TTE and ICE to routine 2D-TTE for the evaluation of the *fossa ovalis* and identification of a PFO. Especially the use of ICE proved to be promising in a clinical setting and has the potential to characterize cardiac anatomy and to guide interventional procedures.

ACKNOWLEDGMENT

Ingrid Vernemmen is a PhD fellow funded by the Research Association Flanders (1556217N).

CONFLICT OF INTEREST DECLARATION

Authors declare no conflict of interest.

OFF-LABEL ANTIMICROBIAL DECLARATION

Authors declare no off-label use of antimicrobials.

INSTITUTIONAL ANIMAL CARE AND USE COMMITTEE (IACUC) OR OTHER APPROVAL DECLARATION

Authors declare no IACUC or other approval was needed.

HUMAN ETHICS APPROVAL DECLARATION

Authors declare human ethics approval was not needed for this study.

ORCID

Ingrid Vernemmen  <https://orcid.org/0000-0002-8185-1450>

Ellen Paulussen  <https://orcid.org/0000-0002-4012-2841>

Annelies Decloedt  <https://orcid.org/0000-0001-8129-2006>

Gunther van Loon  <https://orcid.org/0000-0001-5191-5241>

REFERENCES

- Verheyen T, Decloedt A, Van Der Vekens N, et al. Ventricular response during lungeing exercise in horses with lone atrial fibrillation. *Equine Vet J*. 2013;45(3):309-314.
- Vernemmen I, Vera L, Van Steenkiste G, et al. Reference values for 2-dimensional and M-mode echocardiography in Friesian and warmblood horses. *J Vet Intern Med*. 2020;34(6):2701-2709.
- Decloedt A, De Clercq D, Ven S, et al. Echocardiographic measurements of right heart size and function in healthy horses. *Equine Vet J*. 2017;49(1):58-64.
- Blissitt KJ, Bonagura JD. Pulsed wave Doppler echocardiography in normal horses. *Equine Vet J*. 1995;27(S19):38-46.
- Vandecasteele T, van Loon G, Vandevelde K, de Pauw B, Simoens P, Cornillie P. Topography and ultrasonographic identification of the equine pulmonary vein draining pattern. *Vet J*. 2016;210:17-23.
- Gehlen H, Bubeck K, Stadler P. Pulmonary artery wedge pressure measurement in healthy warmblood horses and in warmblood horses with mitral valve insufficiencies of various degrees during standardised treadmill exercise. *Res Vet Sci*. 2004;77(3):257-264.
- Hallowell GD, Bowen M. Reliability and identification of aortic valve prolapse in the horse. *BMC Vet Res*. 2013;9:9.
- Redpath A, Marr CM, Bullard C, Hallowell GD. Real-time three-dimensional (3D) echocardiographic characterisation of an atrial septal defect in a horse. *Vet Med Sci*. 2020;6(4):661-665.
- Worsman FCF, Miller ZJ, Shaw DJ, Blissitt KJ, Keen JA. Real-time three-dimensional echocardiography for left atrial volume assessment in thoroughbred racehorses: observer variability and comparison with two-dimensional echocardiography. *Equine Vet J*. 2022;54(1):176-190.
- Lang RM, Badano LP, Tsang W, et al. EAE/ASE recommendations for image acquisition and display using three-dimensional echocardiography. *Eur Heart J Cardiovasc Imaging*. 2012;13(1):1-46.
- Long KJ, Bonagura JD, Darke PGG. Standardised imaging technique for guided M-mode and Doppler echocardiography in the horse. *Equine Vet J*. 1992;24(3):226-235.
- Marr CM, Patteson MI. Echocardiography. In: Marr CM, Bowen MI, eds. *Cardiology of the Horse*. 2nd ed. London, UK: Saunders Elsevier; 2010:105-126.
- Enriquez A, Saenz LC, Rosso R, et al. Use of intracardiac echocardiography in interventional cardiology working with the anatomy rather than fighting it. *Circulation*. 2018;137(21):2278-2294.

14. Yastrebov K, Brunel L, Paterson HS, Williams ZA, Bannon PG. Three-dimensional intracardiac echocardiography and pulmonary embolism. *Cardiovasc Ultrasound*. 2020;18(1):1-4.
15. Bartel T, Müller S, Biviano A, et al. Why is intracardiac echocardiography helpful? Benefits, costs, and how to learn. *Eur Heart J*. 2014; 35(2):69-76.
16. Vitulano N, Pazzano V, Pelargonio G, et al. Technology update: Intracardiac echocardiography—a review of the literature. *Med Devices Evid Res*. 2015;8:231-239.
17. Emmert MY, Firstenberg MS, Martella AT, et al. Epicardial left atrial appendage occlusion with a new medical device: assessment of procedural feasibility, safety and efficacy in a large animal model. *J Cardiothorac Surg*. 2020;15:56.
18. Igel DA, Urban JF, Kent JP, et al. Effect of charge delivery on thromboembolism during radiofrequency ablation in canines. *JACC Clin Electrophysiol*. 2018;4(7):958-966.
19. Sayseng V, Grondin J, Salgaonkar VA, et al. Catheter ablation lesion visualization with intracardiac strain imaging in canines and humans. *IEEE Trans Ultrason Ferroelectr Freq Control*. 2020;67(9):1800-1810.
20. Chetboul V, Damoiseaux C, Behr L, et al. Intracardiac echocardiography: use during transcatheter device closure of a patent ductus arteriosus in a dog. *J Vet Cardiol*. 2017;19(3):293-298.
21. Claretti M, Pradelli D, Borgonovo S, Boz E, Bussadori CM. Clinical, echocardiographic and advanced imaging characteristics of 13 dogs with systemic-to-pulmonary arteriovenous fistulas. *J Vet Cardiol*. 2018;20(6):415-424.
22. van Loon G. New frontiers in equine cardiology. *Equine Vet J*. 2018; 50(S52):188-189.
23. Boutet BG, Gordon SG, Navas de Solis C, et al. *Transvenous echocardiography in conscious sedated horses [abstract]*. Seattle, WA: ACVIM Forum; 2018.
24. van Loon G, Van Steenkiste G, Vera L, et al. Catheter-based electrical interventions to study, diagnose and treat arrhythmias in horses: from refractory period to electro-anatomical mapping. *Vet J*. 2020;263: 105519.
25. Schwarzwald CC. Disorders of the cardiovascular system. In: Reed SM, Bayly WM, Sellon DC, eds. *Equine Internal Medicine*. 4th ed. St. Louis, MO: Saunders Elsevier; 2018:387-541.
26. Rana BS, Shapiro LM, McCarthy KP, et al. Three-dimensional imaging of the atrial septum and patent foramen ovale anatomy: defining the morphological phenotypes of patent foramen ovale. *Eur J Echocardiogr*. 2010;11(10):i19-i25.
27. Kutty S, Sengupta PP, Khandheria BK. Patent foramen ovale: the known and the to be known. *J Am Coll Cardiol*. 2012;59(19):1665-1671.
28. Marr CM. Cardiac murmurs: congenital heart disease. In: Marr CM, Bowen MI, eds. *Cardiology of the Horse*. 2nd ed. London, UK: Saunders Elsevier; 2010:193-205.
29. Physick-Sheard PW, Maxie MG, Palmer NC, et al. Atrial septal defect of the persistent ostium primum type with hypoplastic right ventricle in a Welsh pony foal. *Can J Comp Med*. 1985;49(4): 429-433.
30. Schwarzwald CC. Sequential segmental analysis—a systematic approach to the diagnosis of congenital cardiac defects. *Equine Vet Educ*. 2008;20(6):305-309.
31. Silvestry FE, Cohen MS, Armsby LB, et al. Guidelines for the echocardiographic assessment of atrial septal defect and patent foramen ovale: from the American Society of Echocardiography and Society for Cardiac Angiography and Interventions. *J Am Soc Echocardiogr*. 2015;28(8):910-958.
32. Macdonald AA, Fowden AL, Silver M, et al. The foramen ovale of the foetal and neonatal foal. *Equine Vet J*. 1988;20(4):255-260.
33. Baumgartner H, De Backer J, Babu-Narayan SV, et al. 2020 ESC guidelines for the management of adult congenital heart disease. *Eur Heart J*. 2021;42(6):563-645.
34. Blissitt KJ, Young LE, Jones RS, et al. Measurement of cardiac output in standing horses by Doppler echocardiography and thermodilution. *Equine Vet J*. 1997;29(1):18-25.
35. Chuang DY, Sundararajan S, Sundararajan VA, Feldman DI, Xiong W. Accidental air embolism: an uncommon cause of iatrogenic stroke. *Stroke*. 2019;50(7):e183-e186.
36. Collado FMS, Poulin M, Murphy JJ, et al. Patent foramen ovale closure for stroke prevention and other disorders. *J Am Heart Assoc*. 2018;7(12):e007146.
37. Gordon SG, Saunders AB, Achen SE, et al. Transarterial ductal occlusion using the Amplatzer® Canine Duct Occluder in 40 dogs. *J Vet Cardiol*. 2010;12(2):85-92.
38. LeBlanc NL, Agarwal D, Menzen E, et al. Prevalence of major complications and procedural mortality in 336 dogs undergoing interventional cardiology procedures in a single academic center. *J Vet Cardiol*. 2019;23:45-57.
39. Javšica LH, Giguère S, Maisenbacher HW, et al. Percutaneous transcatheter closure of an aorto-cardiac fistula in a Thoroughbred stallion using an Amplatzer occluder device. *J Vet Intern Med*. 2010;24(4): 994-998.
40. Vernemmen I, De Clercq D, Declodet A, et al. Percutaneous transcatheter closure of an aorto-cardiac fistula in a six-year-old Warmblood mare with atrial fibrillation. *J Vet Cardiol*. 2019;24:78-84.

SUPPORTING INFORMATION

Additional supporting information may be found in the online version of the article at the publisher's website.

How to cite this article: Vernemmen I, Paulussen E, Dauvillier J, Declodet A, van Loon G. Three-dimensional and catheter-based intracardiac echocardiographic characterization of the interatrial septum in 2 horses with suspicion of a patent foramen ovale. *J Vet Intern Med*. 2022; 36(4):1535-1542. doi:10.1111/jvim.16451